Competition of interbilayer magnetic couplings in $R_{1.4}Sr_{1.6}Mn_2O_7$ ($R=La_{1-z}Nd_z$)

Y. Moritomo
Center for Integrated Research in Science and Engineering, Nagoya University, Nagoya 464-8601, Japan and PRESTO, JST, Japan

K. Ohoyama and M. Ohashi
Institute for Material Research, Tohoku University, Sendai 980-77, Japan

(Received 7 October 1998)

Chemical substitution effects on the magnetic and transport properties have been investigated for single crystals of $(La_{1-z}Nd_z)_{1.4}Sr_{1.6}Mn_2O_7$ with bilayer structure. We have found that the ferromagnetic ground state for $z=0.0$ is replaced by a layered antiferromagnetic state with alternating ferromagnetic bilayers beyond $z \geqslant 0.1$. Reflecting the subtle balance of the competing interbilayer exchange couplings, application of an external magnetic field induces an antiferromagnetic-ferromagnetic transition. The transition accompanies a switching-type reduction of the current-perpendicular-to-plane resistivity, which can be viewed as a *spin-valve* functionality. [S0163-1829(99)02102-5]

Manganese oxide with cubic perovskite structure has stimulated interest because of their magnetoresistive (MR) properties;[1] they exhibit an extremely large change in resistance in response to applied magnetic field. But for technological applications to magnetic memory or switching device to be viable, great improvements are needed in the field sensitivity. Hwang *et al.* have found a low-field magnetoresistance (MR) in the granular system of cubic manganites and have ascribed the effects to the intergrain tunneling.[2] On the other hands, Sun *et al.*[3] have synthesized a trilayer film of cubic manganites and confirmed a spin-valve functionality.

In contrast, Moritomo *et al.*[4] have found that the doped manganites $(La,Sr)_3Mn_2O_7$ with layered structure shows a large MR near above the insulator-metal transition temperature T_c. In this layered manganite, the MnO_2 sheets are isolated by two La(Sr)O planes, keeping the two-dimensional networks of the MnO_6 octahedra. A low-field magnetoresistance has been reported for crystalline $La_{1.4}Sr_{1.6}Mn_2O_7$ ($x=0.3$) under hydrostatic pressure,[5] even though the magnetic structure remains unknown. This observation suggests the potentialities of the bilayered manganites for applications. Up to the present, extensive studies on the magnetic and lattice structure were performed on $La_{2-2x}Sr_{1+2x}Mn_2O_7$.[6–8] In this system, the hole-doping procedure not only decreases the nominal concentration of the e_g carriers, but significantly release the static Jahn-Teller distortion of the MnO_6 octahedra.[9,10] Such a structural variation affects the magnetotransport properties. In addition, chemical substitution of smaller Nd^{3+} ions for La^{3+} ions also influences the magnetotransport properties. At $x=0.4$, the ferromagnetic metallic state disappears when the Nd^{3+} concentration exceeds 40%.[11] Such chemical pressure effects have been ascribed to the enhanced static Jahn-Teller distortion and the resultant change of the orbital character of the e_g electrons from $d_{x^2-y^2}$-like to $d_{3z^2-r^2}$-like.

In this paper, we have systematically investigated the chemical pressure effect on anisotropic magnetotransport properties for the bilayered manganites, $La_{1.4}Sr_{1.6}Mn_2O_7$ ($x=0.3$). We have determined the magnetic structures by means of neutron powder diffraction measurement, which indicates strong competition between the ferromagnetic and antiferromagnetic interbilayer magnetic couplings. Reflecting a subtle balance between the competing interactions, application of a low magnetic field ($\mu_0 H \sim 0.3$ T) induces an antiferromagnetic-ferromagnetic transition. The current-perpendicular-to-plane (CPP)-MR shows a switching behavior [the MR ratio $\rho_c(0)/\rho_c(H)$ is $\sim 250\%$ at $\mu_0 H=0.3$ T] at the transition, which corresponds to the *open and shut* of the natural spin valve of the local t_{2g} spins (see Fig. 3).

Single crystals of $(La_{1-z}Nd_z)_{1.4}Sr_{1.6}Mn_2O_7$ were grown by the floating-zone method at a feeding speed of 14 mm/h. Stoichiometric mixture of commercial La_2O_3, Nd_2O_3, and $SrCO_3$, and Mn_3O_4 powder was ground and calcined two times at 1300 °C for 24 h. The resulting powder was pressed into a rod with a size of 5 mm$\phi \times$60 mm and sintered at 1350 °C for 48 h. The ingredient could be melted congruently in a flow of air. Large crystals, typically 4 mm in diameter and 20 mm in length, were obtained with two well-defined facets, which correspond to the crystallographic ab-plane. Powder x-ray-diffraction measurements at room temperature and Reitveld analysis[12] indicate that the crystals were nearly single phase. The crystal symmetry is tetragonal ($I4$/mmm; $Z=2$) over the whole concentration range. Obtained lattice parameters are listed in Table I together with the data for $x=0.4$ (cited from Ref. 11). The lattice constant c is much larger as compared with that for $x=0.4$, reflecting the enhanced static Jahn-Teller distortion of the MnO_6 octahedra.[9]

The chemical pressure significantly affects the anisotropic magnetic properties. Figure 1 shows the in-plane (M_{ab}) and out-of-plane (M_c) components of the magnetization curves at 5 K. The magnetization curves at $z=0.0$ indicate that the compound is ferromagnetic with easy axis perpendicular to the MnO_2 sheet. The ferromagnetism as well as the direction of the easy axis were confirmed also by neutron-diffraction study.[13] This makes a sharp contrast with the case of $x=0.4$, in which the easy axis lies in the MnO_2 sheet. Such a varia-

TABLE I. Lattice constants for prototypical bilayered manganites, determined from x-ray powder-diffraction data collected at 300 K. x and z means nominal hole concentration and Nd concentration.

Compound	x	z	a (Å)	c (Å)
$La_{1.4}Sr_{1.6}Mn_2O_7$	0.3	0.0	3.8583(3)	20.304(1)
$(La_{0.95}Nd_{0.05})_{1.4}Sr_{1.6}Mn_2O_7$	0.3	0.05	3.8602(2)	20.325(1)
$(La_{0.9}Nd_{0.1})_{1.4}Sr_{1.6}Mn_2O_7$	0.3	0.1	3.8569(5)	20.317(2)
$(La_{0.8}Nd_{0.2})_{1.4}Sr_{1.6}Mn_2O_7$	0.3	0.2	3.8555(2)	20.318(1)
$(La_{0.7}Nd_{0.3})_{1.4}Sr_{1.6}Mn_2O_7$	0.3	0.3	3.8490(3)	20.296(1)
$La_{1.2}Sr_{1.8}Mn_2O_7$	0.4	0.0	3.8759(3)	20.1496(9)
$Nd_{1.2}Sr_{1.8}Mn_2O_7$	0.4	1.0	3.8345(2)	20.1569(9)

tion of the easy axis is ascribed to the enhanced Jahn-Teller distortion at $x=0.3$, and resultant change of the spin-orbit coupling. At $z=0.1$, a steep peak structure is observed at $T_N=60$ K in the out-of-plane component of susceptibility χ_c (not shown), indicating an antiferromagnetic transition. The out-of-plane component of magnetization M_c gradually increases with field below ~ 0.3 T, and then steeply jumps up to $\sim 3\ \mu_B$ near the ideal value, indicating a metamagnetic transition from antiferromagetic state to ferromagnetic state. On the other hand, the $M_{ab}-H$ curve (filled circles) shows a gradual increase. With further increases of z, the upper critical field $\mu_0 H_{c,u}$ increases from ~ 0.3 T at $z=0.1$ to ~ 6.5 T at $z=0.3$. The large field hysteresis suggests that the metamagnetic transition accompanies a significant lattice structural change.

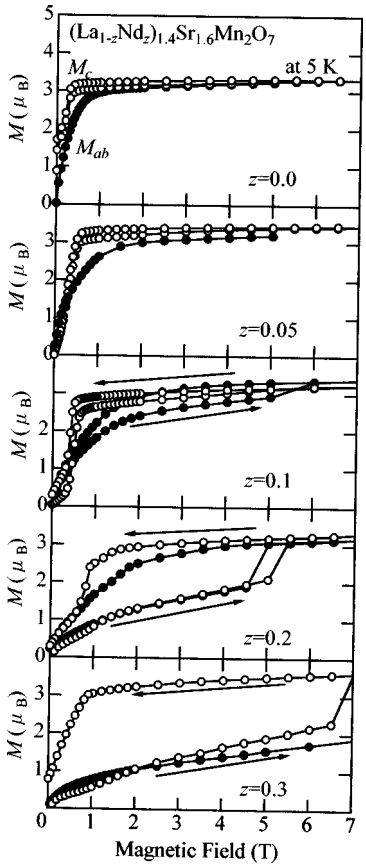

FIG. 1. Anisotropic magnetization curves for $(La_{1-z}Nd_z)_{1.4}Sr_{1.6}Mn_2O_7$ at 5 K. Open and filled circles stand for the out-of-plane (M_c) and in-plane (M_{ab}) components, respectively.

To determine the spin structure of the antiferromagnetic state, we have measured powder neutron patterns for $(La_{0.9}Nd_{0.1})_{1.4}Sr_{1.6}Mn_2O_7$ ($z=0.1$). The powder profiles were obtained with Kinken powder diffractometer for high efficiency and high-resolution measurements, HERMES, installed at the JRR-3M reactor in Japan Atomic Energy Research Institute, Tokai, Japan. Neutrons with wave length 1.819 Å were obtained by the (331) reflection of Ge monochromater, and a combination of 12′-∞-Sample-18′ collimator. Melt-grown crystal ingots were crushed into fine powder and were sealed in a vanadium capsule with helium gas, and mounted at the cold head of the closed-cycle He-gas refrigerator. In Fig. 2 are shown powder patterns at $z=0.1$ together with results of Rietveld refinements (Fat-Rietan[12]); the upper panel is for 100 K ($\geqslant T_N=60$ K) and the lower

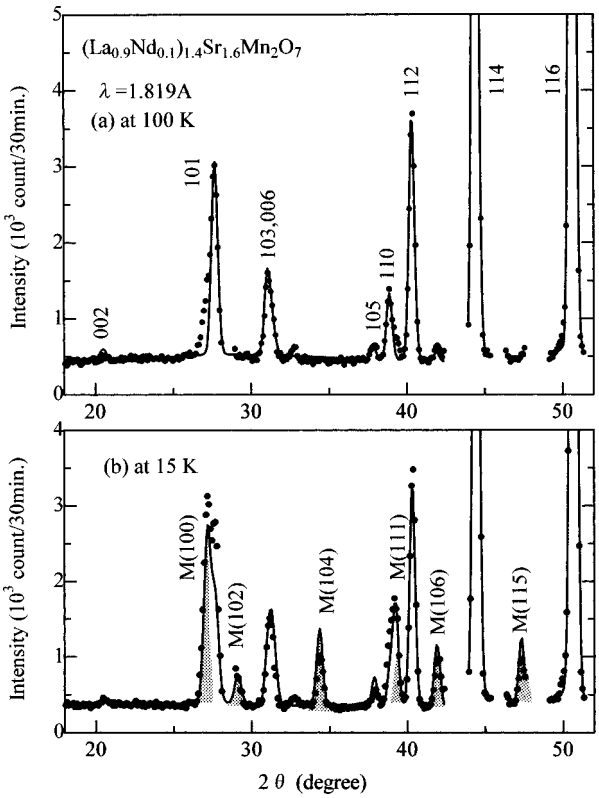

FIG. 2. Neutron powder profiles for $(La_{0.9}Nd_{0.1})_{1.4}Sr_{1.6}Mn_2O_7$ at 100 K ($\geqslant T_N$; upper panel) and 15 K ($\leqslant T_N$; lower panel). Shaded areas indicate magnetic reflections, which are indexed in the $I4/mmm$ setting. The solid curve is the result of the Rietveld refinement ($R_{wp}=10.17$ at 100 K and $R_{wp}=9.34$ at 15 K).

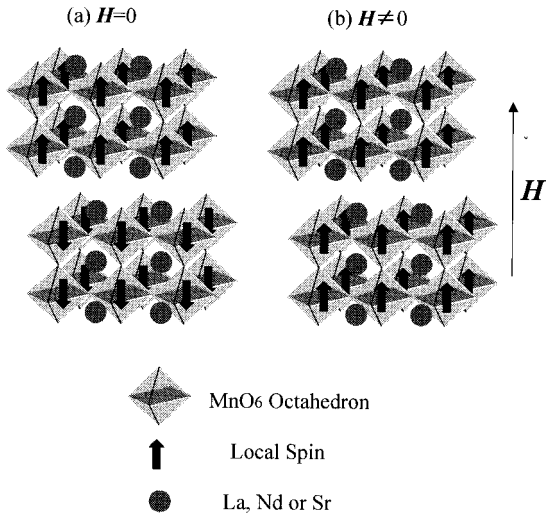

FIG. 3. Schematic lattice and magnetic structures for $(La_{0.9}Nd_{0.1})_{1.4}Sr_{1.6}Mn_2O_7$: (a) without magnetic field and (b) with field along the c direction. Octahedron and thick arrow represent the MnO_6 octahedron and t_{2g} spins, respectively. Gray circles denote the rare-earth (La^{3+} or Nd^{3+}) and alkaline-earth (Sr^{2+}) ions.

panel is for 15 K ($\leqslant T_N$). The lattice parameters are determined to be $a=3.8513(2)$ Å and $c=20.265(1)$ Å at 100 K and $a=3.8520(2)$Å and $c=20.236(2)$ Å at 15 K. The obtained magnetic structure at 15 K is of a layered type, as schematically depicted in Fig. 1(a), with magnetic moment of $3.3\pm0.05\mu_B$ along the c axis. The exchange coupling is ferromagnetic within the bilayer but antiferromagnetic between the neighboring bilayers. The effective transfer integral $t_{\rm eff}$ in the double-exchange system[14] is expressed as

$$t_{\rm eff}=t_0\cdot\cos(\theta/2), \tag{1}$$

where t_0 and θ are bare transfer integral and relative angle of the adjacent t_{2g} spins. Then, the e_g carriers cannot hop into the adjacent bilayers in the layered antiferromagnetic state ($t_{\rm eff}\sim0$ if $\theta\sim\pi$; *shut* state of the spin valve).

In Fig. 4(a) are shown the magnetic phase diagrams determined by the magnetization curves. AFM, FM, and PM denote the antiferromagnetic [see Fig. 3(a)], ferromagnetic [Fig. 3(b)], and paramagnetic state, respectively. The critical fields, $H_{c,i}$ and $H_{c,d}$, are determined from the inflection points of the M_c-H curves in the field-increasing and -decreasing runs, respectively. At $z=0.1$, the layered antiferromagnetic state exists only in the limited region near $H=0$. Application of low magnetic field ($\sim$0.3–0.5 T) along the c direction forcedly aligns the local spins, or *opens* the spin valve [see Fig. 3(b)]. Similar magnetic phase diagrams are obtained for $z=0.2$ [see Fig. 4(b)] and for $z=0.3$. However, the critical field exceeds beyond 1 T.

The subtle balance between the *positive* and *negative* magnetic couplings is considered to be an ascribed structural feature of the $x=0.3$ compound, that is, (1) the large interbilayer spacing ($c/2$; see Table I) and (2) large Jahn-Teller distortion of the MnO_6 octahedra. The increased spacing suppresses the ferromagnetic double-exchange coupling mediated by e_g-carrier hopping, though the coupling slightly overwhelms inherent antiferromagnetic superexchangelike interaction at $z=0.0$. Note that the elongated MnO_6 octahedra along the c direction is advantageous for the inter-bilayer hopping of the e_g carriers, and hence the double-exchange interaction. Such a subtle balance can be inverted by slight structural modification induced by the chemical substitution, and the negative coupling dominates beyond $z=0.1$. Kimura *et al.*[5] have found that application of hydrostatic pressure induces a significant increase of resistivity in the low-temperature state. Judging from the presently investigated chemical pressure effects, the change can be ascribed to the enhanced *negative* exchange coupling and resultant antiferromagnetic spin ordering. It should be mentioned that another type of layered antiferromagnetic structure is observed for the bilayered manganites in the heavily doped region ($x\geqslant0.45$).[9] Contrary to the present case, the magnetic coupling is antiferromagnetic within the bilayer but ferromagnetic between the neighboring bilayers. We have ascribed the intrabilayer antiferromagnetic coupling to formation of the pseudo-two-dimensional band composed of $d_{x^2-y^2}$ orbitals.[9,15]

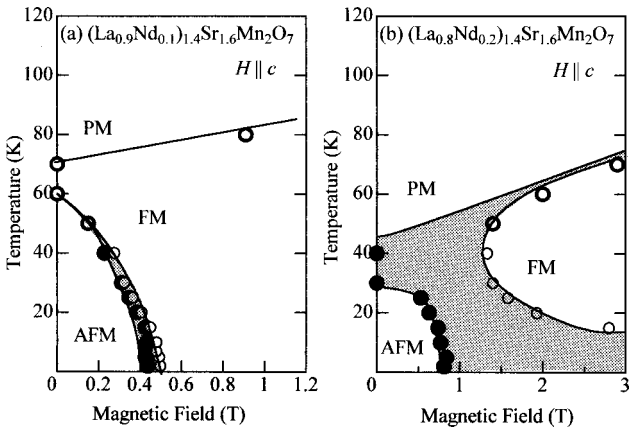

FIG. 4. Magnetic phase diagram for (a) $(La_{0.9}Nd_{0.1})_{1.4}Sr_{1.6}Mn_2O_7$ and (b) $(La_{0.8}Nd_{0.2})_{1.4}Sr_{1.6}Mn_2O_7$. Open and filled circles are the upper ($H_{c,u}$) and lower ($H_{c,l}$) critical field, respectively. AFM, FM, and PM denote antiferromagnetic, ferromagnetic, and paramagnetic states, respectively. Hatched areas stand for bistable regions.

Finally, let us discuss the crucial effect of the magnetic structure (see Fig. 3) on the CPP transport properties. Figure 5 shows magnetic field dependence of out-of-plane component of resistivity ρ_c (upper panel) and magnetization M_c (lower panel) for $(La_{0.9}Nd_{0.1})_{1.4}Sr_{1.6}Mn_2O_7$ at various temperature. Special care has been taken for the quality of the crystal used in the CPP-MR measurement, to avoid any extrinsic effects due to intergrowth or grain boundaries. To improve the crystal quality, we have repeated the necking and seeding procedures six times. The obtained crystal, 3.5 mm in diameter and 20 mm in length, has been checked by neutron-diffraction measurements, and was found to be essentially a single grain with mosaicness less than 0.5°. Large size [$1\times1.5(ab)\times3(c)$mm^3] of the crystal enabled us to measure ρ_c by a conventional four-probe method. Electrical contacts were made with a heat-treatment-type silver paint. On cooling, the ρ_c value increases and shows a local maximum at $\sim$70 K, and then steeply decreases. With further decreasing temperature, a slight upturn is observed below $\sim$40 K. The CCP-MR shows a switching behavior near below the critical magnetic field for the antiferromagnetic-

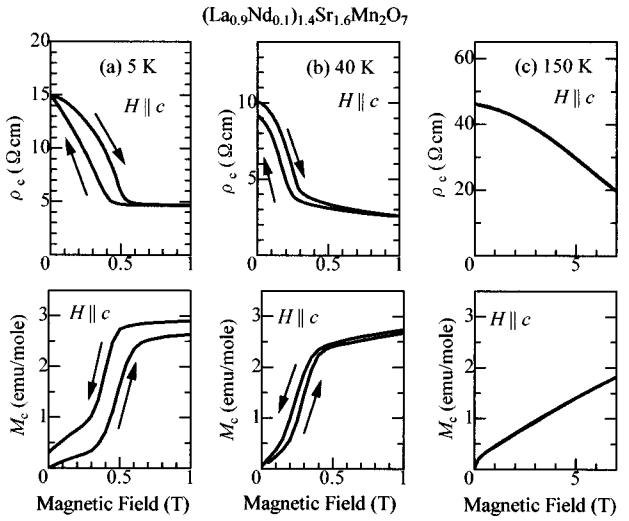

FIG. 5. The current-perpendicular-to-plane magnetoresistance (CPP-MR; upper panel) and corresponding magnetization curve (lower panel) for $(La_{0.9}Nd_{0.1})_{1.4}Sr_{1.6}Mn_2O_7$ at various temperature. The magnetic field was applied perpendicular to the MnO_2 sheet ($H \| c$).

ferromagnetic transition (see also the magnetization curves in the lower panel). For example, at 5 K the CPP resistance decreases from 14 Ω cm down to 4 Ω cm at $H \sim 0.5$ T (in the field-increasing run), and then becomes nearly field independent. The MR ratio defined by $\rho_c(0)/\rho_c(H)$ is ~120% at $H=0.3$ T at 5 K. The ratio further increases up to ~250% ($H=0.3$ T) at 40 K on approaching to T_N ($=60$ K). At 150 K ($\geqslant T_N$), the MR behavior becomes qualitatively different: the ρ_c value decreases with the induced magnetization M_c as $\rho_c(0)$-$\rho_c(H) \propto -M_c^2$, indicating that the MR is of conventional type due to reduced scattering by the local spins.[16]

In summary, we have investigated chemical pressure effects on the magnetotransport properties for $La_{1.4}Sr_{1.6}Mn_2O_7$ with bilayer structure. We have found strong competition between the *positive* and *negative* interbilayer magnetic couplings, which results in the metamagnetic transition accompanied by the noble spin-valve behavior for the CPP-MR. In order to clarify the origin of the interbilayer exchange coupling, detailed investigations on the lattice structure, especially on the distortion of the MnO_6 octahedra, is under progress.

The authors would like to thank A. Nakamura for fruitful discussion and K. Hirota, M. Kubota, Y. Yoshizawa, T. Inami, and K. Nemoto for their help in the neutron-scattering experiment. This work was supported by a Grant-In-Aid for Scientific Research from the Ministry of Education, Science, Sports and Culture, from Precursory Research for Embryonic Science and Technology (PRESTO), Japan Science and Technology Corporation (JST), and from the Mazda Foundation.

[1] For example, S. Jin, T. H. Tiefel, M. McCormack, R. Fastnacht, R. Ramesh, and L. H. Chen, Science **264**, 13 (1994).
[2] H.-Y. Hwang *et al.*, Phys. Rev. Lett. **75**, 914 (1995).
[3] J. Z. Sun *et al.*, Appl. Phys. Lett. **69**, 3266 (1996); J. Z. Sun *et al.*, *ibid.* **70**, 1769 (1997).
[4] Y. Moritomo, A. Asamitsu, H. Kuwahara, and Y. Tokura, Nature (London) **380**, 141 (1996).
[5] T. Kimura, A. Asamitsu, Y. Tomioka, and Y. Tokura, Phys. Rev. Lett. **79**, 3720 (1997).
[6] J. F. Mitchell, D. N. Argyriou, J. D. Jorgensen, D. G. Hinks, C. D. Potter, and S. D. Bader, Phys. Rev. B **55**, 63 (1997).
[7] D. N. Argyriou, J. F. Mitchell, C. D. Potter, S. D. Bader, R. Kleb, and J. D. Jorgensen, Phys. Rev. B **55**, R11 965 (1997); D. N. Argyriou, J. F. Mitchell, J. B. Goodenough, O. Chmaissem, S. Short, and J. D. Jorgensen, Phys. Rev. Lett. **78**, 1568 (1997).
[8] K. Hirota, H. Fujioka, Y. Endo, Y. Moritomo, M. Kubota, and H. Yoshizawa, J. Phys. Soc. Jpn. **67**, 3380 (1997); Y. Moritomo, A. Nakamura, K. Ohoyama, M. Ohashi, and K. Hirota, *ibid.* (to be published).
[9] Y. Moritomo, Y. Maruyama, T. Akimoto, and A. Nakmura, J. Phys. Soc. Jpn. **67**, 405 (1998), and references cited therein.
[10] M. Kubota, H. Yoshizawa, K. Hirota, H. Fujioka, Y. Endo, and Y. Moritomo (unpublished).
[11] Y. Moritomo, Y. Maruyama, T. Akimoto, and A. Nakamura, Phys. Rev. B **56**, R7057 (1997).
[12] F. Izumi, *The Rietveld Method*, edited by R. A. Young (Oxford University Press, Oxford, 1993), Chap. 13.
[13] No antiferromagnetic reflections were observed in the neutron powder-diffraction pattern at 16 K for the melt-grown $La_{1.4}Sr_{1.6}Mn_2O_7$ ($z=0.0$) crystal used in this study. The obtained pattern can be reproduced with ferromagnetic spin structure with a magnetic moment of $2.9 \pm 0.15 \mu_B$ along c axis [M. Kubota *et al.* (unpublished)].
[14] P. W. Anderson and H. Hasagawa, Phys. Rev. **100**, 675 (1955).
[15] T. Akimoto, Y. Maruyama, Y. Moritomo, A. Nakamura, K. Ohoyama, M. Ohashi, and K. Hirota, Phys. Rev. B **57**, R5594 (1998).
[16] A. Urushibara, Y. Moritomo, T. Arima, A. Asamitsu, Y. Tokura, G. Kido, and N. Furukawa, Phys. Rev. B **51**, 14 103 (1995).